Journal of Holography Applications in Physics
Volume 5, Issue 4, Autumn 2025, 27–49
©Available online at http://jhap.du.ac.ir
DOI: 10.22128/jhap.2025.3008.1127
Online ISSN: 2783–3518

Regular article

Mimetic Black Holes in Einstein-Scalar-Gauss-Bonnet Gravity

Maryam Sadeghi[1] · Kourosh Nozari[2]

[1] Department of Theoretical Physics, Faculty of Basic Sciences, University of Mazandaran, P. O. Box–47416–95447, Babolsar, Iran;
Corresponding Author E-mail: m.sadeghio2@umpil.umz.ac.ir

[2] Department of Theoretical Physics, Faculty of Basic Sciences, University of Mazandaran, P. O. Box–47416–95447, Babolsar, Iran;
E-mail: knozari@umz.ac.ir

Received: August 3, 2025; **Revised:** September 14, 2025; **Accepted:** September 14, 2025

Abstract. In this paper, we try to extend the intriguing concept of mimetic black holes to the realm of the Gauss-Bonnet Gravity. Mimetic black holes are a fascinating theoretical construct that mimic the exterior gravitational field of known black holes even without possessing an event horizon in some specific conditions. By incorporating the Gauss-Bonnet theory, we aim to investigate how the dynamics and properties of mimetic black holes are altered in this modified gravitational framework. In this particular setting, we explore the existence of black hole solutions with nontrivial scalar hair while being influenced by the mimetic scalar field in the Einstein-Scalar-Gauss-Bonnet (ESGB) theory. These solutions are characterized by their regularity and offer new insights into the dynamics of black holes in this theory. We proceed by conducting an analytical study in the near horizon asymptotic regime when an event horizon cab be existed. Our analysis reveals that in this setup a black hole event horizon with a nontrivial hair can be formed, regardless of the sign of the Lagrange multipliers λ, depending on the particular selection of the coupling between the scalar field and the Gauss-Bonnet term. Notably, this black hole horizon remains regular, emphasizing the robustness of the black hole solutions in this setup.

Keywords: Mimetic Gravity; Einstein-Scalar-Gauss-Bonnet Theory; Black Holes; Near-Horizon Geometry

Contents

1 Introduction

Modern cosmology faces a significant issue in understanding the nature of the Universe's dark contents, which account for $\sim 95\%$ of the total mass-energy budget. According to Ref. [1–3], the dark side of the Universe is made up of two components: dark energy ($\sim 69\%$) and dark matter ($\sim 26\%$) of the mass-energy content. The Universe's expansion is positively accelerated by the former's antigravity property and negative pressure, whereas the latter adds to gravity but not electromagnetic interaction. Dark matter is also required to explain the observed motions of galaxies and clusters, as baryonic matter alone cannot generate sufficient gravitation. Dark matter contributes significantly to the cosmic microwave background anisotropies, galaxy cluster velocity dispersion, large-scale structure distributions, gravitational lensing, and X-ray measurements from galaxy clusters. It's feasible to approach the situation differently. Some physicists think that dark matter is a manifestation of a gravity theory beyond General Relativity, rather than a particle-based phenomenon. Modified gravity theories have been proposed to explain gravitational lensing, flat rotation curves of galaxies, and cluster dynamics through geometrical effects. Nearly a decade ago, the Mimetic Theory of Gravity was proposed as an alternative explanation for the dark matter puzzle [4]. The mimetic field can add an extra degree of freedom to the gravitational field. The gravitational field has both transverse and longitudinal degrees of freedom, potentially mimicking dark matter. A modified form of mimetic gravity has been shown to resolve both cosmological singularities [5] and black hole singularities [6]. The mimetic theory predicts that gravitational waves (GW) propagate at the speed of light, which is consistent with the results of the event GW170817 and its optical counterpart [7,8]. This theory can explain spiral galaxies' flat rotation curves [9] and dark energy problem [10]. In recent years the issue of black hole physics and thermodynamics has attracted even much more attentions, see for instance [11] and references therein. In this respect looking at black holes physics from the lens of mimetic gravity is interesting. The research on mimetic gravity were also generalized to $f(R)$ gravity [12,13], braneworld gravity [14–18] and Gauss-Bonnet gravity [19,20] towards a unified description from the early cosmological inflation to the late-time cosmic speed up under mimetic scenario.

In mimetic gravity theory, the conformal degree of freedom of the gravitational field can be separated by introducing a new relationship as (see Ref. [4])

$$g_{\alpha\beta} = \mp(\bar{g}^{\mu\nu}\partial_\mu\phi\partial_\nu\phi)\bar{g}_{\alpha\beta}\,, \tag{1.1}$$

where $g_{\alpha\beta}$ is the physical metric, $\bar{g}_{\alpha\beta}$ is the auxiliary metric and ϕ is the scalar field [7,8]. The first attempt to find a satisfactory black hole solution in mimetic gravity was conducted by Gorji et al. [21]. In a previous research [10], it has been shown that the mimetic constraint is inconsistent with the black hole geometry that includes horizons. To remove this discrepancy, the constraint (1.1) is adjusted by integrating the function $\omega(\phi)$ or the auxiliary field λ as a Lagrange multiplier or by both of them in the following approaches [22]

$$\omega(\phi)g^{\alpha\beta}\partial_\alpha\phi\partial_\beta\phi = \pm 1, \tag{1.2}$$

$$\lambda(g^{\mu\nu}\partial_\mu\phi\partial_\nu\phi \pm 1) = 0, \tag{1.3}$$

$$\lambda(\omega(\phi)g^{\rho\sigma}\partial_\rho\phi\partial_\sigma\phi + 1) = 0. \tag{1.4}$$

This leads to the solutions for static mimetic black holes, time-dependent mimetic black holes, and black holes in an expanding universe. Sometimes, they are presented as solutions both inside and outside the black hole. On the other hand, the scientific literature is still full of interest in generalized gravitational theories because the ultimate theory of quantum gravity, which would enable the unification of gravitational interactions with other forces and robustly describe them at high energies, is still elusive. These theories provide the framework within which several solutions of the traditional General Relativity (GR) have been re-examined. They include extra fields or higher-curvature terms in their action [23].

Accordingly, scalar field based generalized gravitational theories were among the first to be investigated. The search for new black-hole solutions, which went beyond the three widely recognized families of general relativity, was abruptly put on hold when the no-hair theorem [24] was developed. This theorem prohibited the possibility of a static solution of this type that had a non-trivial scalar field related to it. However, counter-examples such as black holes with Skyrme fields [25], Yang-Mills [26], or a conformal coupling to gravity [27] emerged in the years that followed. In 1995, a new formulation of the no-hair theorem was put out [28]; however, this was also circumvented a year later when dilatonic black holes were discovered in relation to the Einstein-Dilaton-Gauss-Bonnet theory [29]. The second wave of black-hole solutions was obtained within the framework of superstring theory-inspired theories [30]. However, the revived development of the Horndeski [31] and Galileon [32] ideas within the past ten years has greatly expanded the building of generalized gravitational theories. As a result, new formulations of the no-hair theorems covering the scenarios of Galileon fields [33] and standard scalar-tensor theories [34] were proposed. Nevertheless, in Ref. [4] these more modern forms were also avoided, and in Ref. [35] some concrete black-hole solutions were obtained. More recently, it was almost simultaneously shown by three different groups [36] that innovative black-hole solutions with a non-trivial scalar hair may be admitted a generalized gravitational theory containing a scalar field and the quadratic Gauss-Bonnet (GB) term.

It was demonstrated in a general theoretical argument in Ref. [37] that the GB term's presence is crucial for avoiding the innovative no-hair theorem. Furthermore, the exact form of the coupling function $f(\phi)$ between the GB term and the scalar field has no effect on the emergence of the solutions: an asymptotic solution describing a regular black-hole horizon with a non-trivial scalar field could always be constructed as long as the first derivative of the scalar, ϕ_r^h, at the horizon obeys a particular constraint. Thus, a variety of coupling functions $f(\phi)$ forms were employed to determine a large number of asymptotically flat black hole solutions with scalar hair [35]. Additional studies presenting novel black holes or compact objects solutions in generalized gravitational theories have reported [38,39], as well as further studies of the properties of these novel solutions [40]. In this streamline of research, here we aim to explore at least some uncovered features of the concept of mimetic black holes in the framework of the Scalar-Einstein-Gauss-Bonnet gravity. The reasons for adopting such a relatively complicated framework is the fact that understanding the low-energy limit of string theory has been the subject of a notable number of attempts in higher dimensions gravity in the last few decades. An extremely significant higher dimensional generalization of Einstein's gravity is the Einstein–Gauss Bonnet gravity which David Lovelock [41] later rediscovered after Lanczos [42] made the suggestion. The Study of the Einstein-Gauss-Bonnet (EGB) theory becomes crucial because it offers a more comprehensive understanding of the setup to investigate numerous conceptual problems pertaining to gravity. This theory is devoid of all ghost and the Einstein-Gauss-Bonnet theory's field equations' order are not higher than two. Boulware and Deser were the first to obtain the exact black hole solution in the Einstein Gauss-Bonnet gravity, despite numerous attempts to do so since their inception [43]. Subsequently, several researchers have examined numerous precise black hole solutions together with their thermodynamical characteristics [44–46]. There have also been investigations into a number of black hole solutions with matter sources that generalize the Boulware–Desser solution [47,48]. In this work we investigate the effects on the dynamics and properties of mimetic black holes [21] in EGB gravity. This investigation will contribute a small step toward our comprehension of the interplay between gravity and the fundamental laws of nature, potentially unraveling fresh insights into the essence of black holes and the structure of space-time itself in a mimetic viewpoint.

The primary objective of our study is to derive the metric of a mimetic black hole embedded in the Einstein-Gauss-Bonnet theory and subsequently try to compute its event horizon radii following the strategy adopted in [19,49] but in a mimetic framework. It is worth mentioning that the constructed setup has some connection with holography and AdS/CFT correspondence. Mimetic field follows essentially the gauge/gravity duality and it is natural to expect some traces of holography via AdS/CFT correspondence in this context, especially when one deals with black holes as prominent candidate for manifestation of the holography idea. The results of this study, focused on the asymptotically flat black holes, provide the groundwork for several intriguing possibilities within the context of the AdS/CFT correspondence. While speculative, the extensions and interpretations outlined below highlight the potential relevance of the mimetic-Gauss-Bonnet gravity to holography. **1**-Holographic Dual of Mimetic Hair: The primary feature of our solutions is the nontrivial, regular scalar hair supported by the combined effects of the mimetic constraint and the Gauss-Bonnet coupling. In a hypothetical asymptotically AdS extension of this model, this scalar hair would be dual to a scalar operator O_ϕ in the boundary conformal field theory (CFT). The mimetic constraint, which is inherently geometric, would likely impose a novel relation between this operator and the stress-energy tensor $T_{\mu\nu}$ of the boundary theory. Studying the properties of this operator- its scaling dimension, correlation functions, and its backreaction on the thermal state- could reveal new strongly coupled quantum phenomena [50,51]. **2**-Mimetic Gravity as an Effective Theory for Holographic Renormalization Group (RG) Flows: The mimetic field can be interpreted as a preferred spacetime foliation. In holography, the radial direction in AdS corresponds to the energy scale of the dual field theory via the renormalization group (RG) flow. A natural extension would be to study our system in an AdS background, where the mimetic scalar ϕ could define a specific holographic slicing. This might provide a gravitational description of RG flows with a built-in "reference scale", potentially offering new insights into the dynamics of confinement, deformation, or the emergence of geometry from entanglement [52–55]. **3**-Regularization of Holographic Singularities: Our analysis showed that the inclusion of the Gauss-Bonnet term resolves the caustic singularity present in pure mimetic black hole solutions, leaving only the central curvature singularity. In holography, singularities in the bulk often signal limitations in the effective field theory description of the boundary. Investigating whether this mechanism can be extended to soften other types of singularities in AdS- for example, those inside holographic superconductors or during thermal quenches- could be valuable. A mimetic-Gauss-Bonnet model in AdS might provide a framework for constructing holographic duals with improved UV behavior [56,57]. **4**-Holographic Thermodynamics and Phase Structure: The modified entropy formula we derived, that is, $S_h = A_h/4 + 4\pi f(\phi)$, directly impacts the black hole thermodynamics. In an AdS setting, black holes undergo rich phase transitions (e.g., Hawking-Page transitions). The mimetic field, influencing the entropy and temperature, could significantly alter this phase diagram. Studying the phase structure of mimetic-Gauss-Bonnet black holes in AdS would be a direct and fascinating application, with the boundary interpretation being a transition between confined and deconfined phases in a dual field theory with unusual thermodynamic properties [58–62].

With these preliminaries, the present manuscript is organized as follows: In the next section we utilize the gravitational field equations and the equation for the mimetic scalar field. Thus, by exploring the possibility of an asymptotic solution within the field equations outlined in the references, we develop approaches to mimetic black hole solutions following the seminal work [63]. These solutions provide a detailed description of a regular black hole horizon [64,65]. Specifically, our goal is to ascertain whether the field equations permit an asymptotic solution that exhibits a well-behaved black hole horizon. In this EGB mimetic theory, we additionally explore how the shape of the asymptotic solution of the field equations far away from the event horizon of a black hole is influenced by the sign of the mimetic factor λ. By examining the dependence on the mimetic coefficient λ and the coupling function $f(\phi)$, we seek to gain insights into the behavior attributed to mimetic black hole solutions in this setup.

2 Theoretical Framework

In this paper, we delve into a broad category of gravitational theories which include additional higher curvature terms alongside a mimetic scalar field. The action functional for these theories is defined as follows (with $8\pi G = 1 = c$):

$$S_{\pm} = \int d^4x\sqrt{-g}\left[\frac{R}{2} + f(\phi)R^2_{GB} + \lambda(g^{\mu\nu}\partial_\mu\phi\partial_\nu\phi \mp 1)\right] , \tag{2.1}$$

where

$$R^2_{GB} = R_{\mu\nu\rho\sigma}R^{\mu\nu\rho\sigma} - 4R_{\mu\nu}R^{\mu\nu} + R^2 , \tag{2.2}$$

is commonly referred to as the Gauss–Bonnet term [66]. R represents the Ricci scalar, $f(\phi)$ represents a universal coupling function. The mimetic field plays a vital role in enhancing the field equations λ is the auxiliary field (Lagrange multiplier) that enforces the mimetic constraint equation [4,22]:

$$g^{\mu\nu}\partial_\mu\phi\partial_\nu\phi = \pm 1 . \tag{2.3}$$

In relation to the sign $\mp$ of the action in (2.1), we should mention that depending on the nature of the system, since the interior of the black hole is not static and depends on time, the negative sign $(-)$ must be used in the mimetic transformation. This means that the derivative vector of the scalar field is a time-like vector. In the case of static solutions, such as the space outside the black hole, the positive sign $(+)$ should be considered. In this case, the derivative vector of the scalar field becomes space-like. These are two possible solutions; however the S_+ solution is consistent with the static and the S_- solution leads to an imaginary scalar field, which is not physically meaningful in this context [21].

In our analysis, we consider a static and spherically-symmetric mimetic scalar field. The coupling function $f(\phi)$ will be kept undetermined in the initial steps of our examination. However, at the stage of deriving specific solutions numerically, a particular form for $f(\phi)$ will be chosen, with respect to the metric tensor $g^{\mu\nu}$ and the scalar field ϕ.

As emphasized in earlier works, the coupling function $f(\phi)$ plays a central role in enabling scalar-tensor interactions, particularly in scenarios that give rise to black-hole solutions with non-trivial scalar hair [67,68]. Previous research has demonstrated that the inclusion of the Gauss-Bonnet (GB) term plays a main role in evading the novel no-hair theorem. Based on this, a broad class of asymptotically flat black-hole solutions with non-trivial scalar hair have been obtained for a wide variety of coupling functions $f(\phi)$. The coupling function $f(\phi)$ serves as a crucial link between the scalar field ϕ and the GB term in the gravitational action. It acts as an intermediary that enables the scalar field to interact with the curvature of space-time. Remarkably, the existence of these hairy black-hole solutions does not depend sensitively on the specific form of $f(\phi)$ rather, it is the mere presence of such a coupling that allows scalar hair to be sustained [67,68].

By varying the action (2.1) with respect to the metric tensor $g_{\mu v}$ and the scalar field ϕ, both the gravitational field equations and the equation for the mimetic scalar field can be derived as follows: (with $8\pi G = 1 = c$)

$$G_{\mu\nu} = T_{\mu\nu}\,, \tag{2.4}$$

$$\dot{f}(\phi)R^2_{GB} - 2\nabla_\mu(\lambda(\partial^\mu\phi)) = 0\,, \tag{2.5}$$

where $G_{\mu\nu}$ is the Einstein tensor and $T_{\mu\nu}$ is the energy-momentum tensor, written as follows

$$T^{(1)}_{\mu\nu} = -2\lambda(\partial_\mu\phi\partial_\nu\phi) + g_{\mu\nu}\lambda(\partial_\rho\phi\partial^\rho\phi \mp 1)\,, \tag{2.6}$$

$$T^{(2)}_{\mu\nu} = -\left(g_{\rho\mu}g_{\lambda\nu} + g_{\lambda\mu}g_{\rho\nu}\right)\eta^{\kappa\lambda\alpha\beta}\tilde{R}^{\rho\gamma}_{\alpha\beta}\nabla_\gamma\partial_\kappa f(\phi)\,, \tag{2.7}$$

with

$$T_{\mu\nu} = T^{(1)}_{\mu\nu} + T^{(2)}_{\mu\nu}\,. \tag{2.8}$$

In the above equations, a dot over the coupling function denotes its derivative with respect to the scalar field (i.e. $\dot{f} = \frac{df}{d\phi}$). We have also used the definition:

$$\tilde{R}^{\rho\gamma}_{\alpha\beta} = \eta^{\rho\gamma\sigma\tau}R_{\sigma\tau\alpha\beta} = \frac{\epsilon^{\rho\gamma\sigma\tau}}{\sqrt{-g}}R_{\sigma\tau\alpha\beta}\,. \tag{2.9}$$

In this study, we investigate the emergence of regular, static, spherically symmetric black hole solutions and characteristics of a non-trivial mimetic scalar field. Accordingly, the line-element describing the regular, static, asymptotically flat black hole will be expressed as follows:

$$ds^2 = -e^{A(r)}dt^2 + e^{B(r)}dr^2 + r^2\left(d\theta^2 + \sin^2\theta d\phi^2\right)\,. \tag{2.10}$$

By utilizing this line-element, it is straightforward to determine the non-vanishing components of the Einstein tensor $G_{\mu\nu}$ as:

$$G^t_t = \left(\frac{e^{-B(r)}}{r^2}\right)\left(-B'r - e^{B(r)} + 1\right)\,, \tag{2.11}$$

$$G^r_r = \left(\frac{e^{-B(r)}}{r^2}\right)\left(A'r - e^{B(r)} + 1\right)\,, \tag{2.12}$$

$$G^\theta_\theta = \left(\frac{e^{-B(r)}}{4r}\right)\left(A'^2r + 2A''r + A'(2 - rB') - 2B'\right)\,, \tag{2.13}$$

$$G^\phi_\phi = \left(\frac{e^{-B(r)}}{4r}\right)\left(A'^2r - A'rB' + 2A''r + 2A' - 2B'\right)\,. \tag{2.14}$$

In the mimetic gravity framework, Einstein's theory of gravity is reformulated in a way that isolates the conformal degree of freedom in a covariant manner. This is achieved by introducing a physical metric that is defined in terms of an auxiliary metric and a scalar field, which appears through its first derivatives [69,70]. The conformal transformation relating the physical metric $g_{\mu\nu}$ to the auxiliary metric $\tilde{g}_{\mu\nu}$ and the scalar field ϕ is given by:

$$g_{\mu\nu} = \pm(\tilde{g}^{\alpha\beta}\partial_\alpha\phi\partial_\beta\phi)\tilde{g}_{\mu\nu}\,. \tag{2.15}$$

Also, the variation of the action functional with respect to the auxiliary field λ yields the following relationship [64]:

$$\frac{\partial S_\pm}{\partial\lambda} = 0 \to g^{\mu\nu}\partial_\mu\phi\partial_\nu\phi = \pm 1\,. \tag{2.16}$$

Constraint (2.16) may take the form of a second-order polynomial which can be solved to find e^B. The rr component of Einstein's equations yields:

$$e^B = \phi'^2 \,, \tag{2.17}$$

so that,

$$B' = 2\frac{\phi''}{\phi'} \,. \tag{2.18}$$

We are interested in asymptotic flat solutions, so as $r \to \infty$ we have $e^A \to 1$ and $e^B \to 1$ (see Figure 1). Nevertheless, it becomes evident that the inclusion of the mimetic constraint significantly influences not only the asymptotic solutions but also the characteristics and even the existence of the resulting black holes solution. In our examination, we utilize a prime symbol to denote differentiation with respect to the variable r. Based on the obtained relations for the metric functions, we can rewrite the energy-momentum tensor as follows:

$$T_t^t = \frac{r^2\lambda(r) - 4\ddot{f}}{r^2} - \lambda(r) + \frac{4\ddot{f}}{r^2\phi'^2} - \frac{8\dot{f}\phi''}{r^2\phi'^4} \,, \tag{2.19}$$

$$T_r^r = -2\lambda(r) - \frac{2\dot{f}A'}{r^2\phi'} + \frac{6\dot{f}A'}{r^2\phi'^3} \,, \tag{2.20}$$

and

$$T_\phi^\phi = T_\theta^\theta = \frac{2\ddot{f}A'}{r\phi'^2} + \frac{4\dot{f}A'^2 + 8\dot{f}A''}{4r\phi'^3} - \frac{4\dot{f}\phi''A'}{r\phi'^4} \,. \tag{2.21}$$

The Einstein tensor is rewritten to match the above relations [41]. By identifying the components of $G_{\mu\nu}$ and $T_{\mu\nu}$, we can determine the specific form of Einstein's field equations. These equations are also supported by the scalar-field equation (2.5), which can be explicitly expressed as follows:

$$\begin{aligned} &\frac{4\left(A'' + \left(\frac{A'\left(A' - 6\frac{\phi''}{\phi'}\right)}{2}\right)\right)\dot{f}}{\phi'^2} + 4A''\dot{f} + 2r^2\phi''\lambda(r) + 2A''^2\dot{f} \\ &+ \left(r^2\lambda(r)\phi' - \frac{4\dot{f}\phi''}{\phi'}\right)A' + 2\phi' r\left(-\frac{\lambda(r)\phi'' r}{\phi'} + \lambda' r + 2\lambda(r)\right) = 0 \,. \end{aligned} \tag{2.22}$$

By utilizing the line-element (2.10), Einstein's equations can be explicitly formulated as follows:

$$\frac{-\phi'^3 - 2\phi'' r + \phi'}{r^2\phi'^3} = \frac{-\ddot{f}\phi'^4 + 4\ddot{f}\phi'^2 - 8\dot{f}\phi''}{r^2\phi'^4} \,, \tag{2.23}$$

$$\frac{-1}{r^2} - \frac{A'r + 1}{r^2\phi'^2} = -2\lambda - \frac{2\dot{f}A'(\phi'^2 - 3)}{r^2\phi'^3} \,, \tag{2.24}$$

and

$$\frac{(-2A'r - 4)\phi'' + \phi'(A'^2 r + 2A'' r + 2A')}{4r\phi'^3} = \frac{1}{r\phi'^4}\left[A'^2\phi'\dot{f} + 2A'\phi'^2\ddot{f} - 4A'\phi''\dot{f} + 2\phi'\ddot{f}A''\right] \,. \tag{2.25}$$

After deriving the main equations of the setup, we pay attention to the solutions of these equations. Since these are very complicated equations, analytical, closed-form solutions are not available and we have to follow some simplifications, asymptotic solutions and numerical analysis.

At this stage some discussion about existence of the horizons in this setup is worth mentioning.

As has been shown in original work on mimetic black holes by Gorji et al., (Ref. [21]), obtaining an analytical (event) horizon radius for a static black hole solution in the pure mimetic gravity scenario is not an easy task. This is because unlike in cosmological setups where one uses only a timelike vector, here in mimetic scenario one needs both timelike and spacelike vectors constructed via the derivatives of the mimetic field to fix the location of the horizon(s). Nevertheless, as has been discussed in Ref. [21], in some special circumstances there are horizons of the types apparent, Killing or event horizon. In fact, in the setup of Ref. [21], one does not obtain a true event horizon as in the Schwarzschild case. If the mimetic field is switched off in the background (that is, $\lambda = 0$ in Ref. [21]), one simply recovers the Schwarzschild solution, and the usual event horizon at $r = 2m$ is present. However, once the mimetic scalar contributes ($\lambda \neq 0$), the static solution loses the horizon completely and results in naked singularities. To rescue something resembling a black hole, the authors in Ref. [21] glue an exterior solution to an interior one, and the surface at $r = 2m$ behaves only as an apparent horizon- not a true event horizon.

In our more involved setup due to the presence of GB effect, it is possible essentially to find event horizon with the same technique. However, due to the complication of constructed model, no analytical solution for the horizon radius is possible. So, we restricted ourselves to a numerical study of the issue in present context. In fact, in this manuscript we study black holes within mimetic EGB gravity theory, which is more involved in comparison with the genuine mimetic black hole studied in Ref. [21] and our solutions explicitly are capable to realize event horizon. So, the solutions we present and analyze are capable to admit a regular event horizon. Our entire asymptotic analysis in the next Section is predicated on the existence of a horizon at some radius $r = r_h$, where $e^{A(r)} \to 0$ and $e^{B(r)} \to \infty$. The analytical and numerical results confirm that such a structure can consistently emerge from the field equations in this theory. In summary, in our Mimetic Einstein-Scalar-Gauss-Bonnet (ESGB) setup it is possible to obtain solutions with a genuine event horizon, but we should stress that it is not guaranteed automatically. Whether the horizon is an actual event horizon (a global causal boundary) or only an apparent/coordinate/caustic-type horizon depends on the details of coupling function, $f(\phi)$, the boundary/regularity conditions at the would-be horizon, and the global extension of the solution. In what follows we elaborate this last statement. The Gauss-Bonnet coupling in our Mimetic EGB setup, $f(\phi)$, frequently enables scalar-hairy black holes in ESGB models (this is a well-known issue); the higher-curvature term allows nontrivial scalar profiles while still admitting regular metric horizons. Thus, adding a mimetic scalar on top of the ESGB does not a priori forbid the existence of the event horizons - in fact, the GB coupling often helps form hairy solutions with a regular horizon. We constructed the near-horizon asymptotic conditions by demanding the conditions $e^{A(r)} \to 0$ and $e^{B(r)} \to \infty$ and bounded ϕ as $r \to r_h$. We then derive algebraic/ODE relations (the expressions for A'', ϕ', the discriminant $C \geq 0$, and for $\lambda(r)$). These relations demonstrate that there exist parameter regions and choices where the near-horizon expansions are self-consistent, i.e., a regular horizon is permitted by the field equations. The imposed conditions (metric component behavior and bounded scalar field) are local near r_h. A local regular horizon can correspond to an event horizon, but proving it is indeed a global event horizon requires causal analysis of the full solution (extension across the horizon, null geodesic completeness and escape to infinity, and the absence of future-directed causal curves from inside to outside). We emphasize that our asymptotic analysis is therefore a necessary step, but not a complete proof of the existence of a global event horizon.

2.1 Asymptotic Solutions at the Black Hole Horizon

In our quest to derive novel black-hole solutions, we will first examine whether the field equations allow for an asymptotic solution that describes a regular black-hole horizon. With the discussions at end of the previous part, rather than making the typical power-series assumption with respect to $r - r_h$, where r_h represents the horizon radius, we develop the solution using the same method as has been adopted in earlier research such as the Ref. [63,68]. Specifically, we demand that, as we approach the horizon, the metric function e^A should approach zero while e^B approaches infinity, and the scalar field must stay bounded.

To satisfy these conditions, we assume that A' diverges as $r \to r_h$, a point we will justify subsequently, while ϕ' and ϕ'' remain finite in the same limit.

We can formulate a set of two separate, second-order coupled differential equations for the corresponding functions A'' and ϕ'' in the following manner

$$\begin{aligned} A''(r) =& -\frac{\phi''(2\phi'^2\lambda(r)r^2 - \phi'^2 + 1)}{2\dot{f}\phi'^2 + \phi' r - 6\dot{f}} - \frac{\phi'(4\phi'\lambda(r)r^2\phi'' + 2\phi'^2\lambda'(r)r^2 + 4\phi'^2\lambda(r)r - 2\phi'\phi'')}{2\dot{f}\phi'^2 + \phi' r - 6\dot{f}} \\ & + \frac{1}{(2\dot{f}\phi'^2 + \phi' r - 6\dot{f})^2}\Big(\phi'(2\phi'^2\lambda r^2 - \phi'^2 + 1)(2\dot{f}\phi'^3 + 4\dot{f}\phi'\phi'' + \phi'' r + \phi' - 6\ddot{f}\phi')\Big)\,, \end{aligned} \tag{2.26}$$

$$\begin{aligned} \phi'(r) =& \frac{(324\lambda^2\dot{f}r^4A' + 18\lambda\dot{f}r^3A'^2 - 8\dot{f}^3A'^3 + 6\sqrt{3C}\lambda r^2 - 306\lambda\dot{f}r^2A' - 9\dot{f}rA'^2 - 3\sqrt{3C} + 72\dot{f}A')^{\frac{1}{3}}}{6r^2\lambda - 3} \\ & - \frac{6\lambda r^3A' - 4\dot{f}^2A'^2 + 6r^2\lambda - 3A'r - 3}{(6r^2\lambda - 3)(\dot{f}(324\lambda^2r^4A' + 18\lambda r^3A'^2 - 8\dot{f}^2A'^3 - 306\lambda r^2A' - 9rA'^2 + 72A') - 3\sqrt{3C} + 6\sqrt{3C}\lambda r^2)^{\frac{1}{3}}} \\ & - \frac{2\dot{f}A'}{6r^2\lambda - 3}\,, \end{aligned} \tag{2.27}$$

where by definition

$$\begin{aligned} C \equiv& 972\lambda^2\dot{f}^2r^4A'^2 + 108\lambda\dot{f}^2r^3A'^3 + 2\lambda r^5A'^3 - 48\dot{f}^4A'^4 - \dot{f}^2r^2A'^4 - 864\lambda\dot{f}^2r^2A'^2 + 6\lambda r^4A'^2 \\ & - 56\dot{f}^2rA'^3 - r^3A'^3 + 6\lambda r^3A' + 188\dot{f}^2A'^2 - 3r^2A'^2 + 2r^2\lambda - 3A'r - 1\,. \end{aligned} \tag{2.28}$$

The quantity C within the square root symbolizes an exact combination and must always be positive or zero for the expression to have a real solution, that is, $C \geq 0$.

The positivity of the expression C indicates that

$$\begin{aligned} \phi(r) =& \Upsilon + \frac{1}{2}\ln\Bigg[\left(\frac{1}{A'^2}\right)\Bigg(-\sqrt{(6r^2\lambda + A'r - 2)(54r^2\lambda + A'r - 26)^3} \\ & - r^2A'^2 + (108r^3\lambda - 56r)A' + 972\lambda^2r^4 - 864r^2\lambda + 188\Bigg)\Bigg]\,, \end{aligned} \tag{2.29}$$

where Υ is a negative constant. From the analytical solutions of equation (2.24), the value of A is determined as follows:

$$A(r) = \int -\frac{\phi'(2\phi'^2\lambda(r)r^2 - \phi'^2 + 1)}{2\dot{f}\phi'^2 + \phi' r - 6\dot{f}}dr + C_1\,. \tag{2.30}$$

Here C_1 is another integration constant. Due to the high complexity of the field equations, we cannot provide an exact analytical and explicit solution to this equation. This relation is exact and one of our main results which exclusively determines the behavior of the metric function e^A in the vicinity of the event horizon.

Equations that include the mimetic constraint and general coupling function facilitate the formation of a black-hole solution with a regular horizon. The values of λ are obtained by solving the equation (2.24) as follow:

$$\lambda(r) = \frac{1}{2r^2} - \frac{A'r+1}{2r^2\phi'^2} - \frac{\dot{f}A'}{r^2\phi'} + \frac{3\dot{f}A'}{r^2\phi'^3}\,. \tag{2.31}$$

The behavior of λ as the mimetic coefficient at the different radial distances from the horizon of the black hole will be shown in forthcoming arguments. We shall discuss and justify the numerical results just after a look at the thermodynamic aspects of the mimetic black hole solution in this EGB setup.

3 Thermodynamic Analysis

In this section, we delve into the thermodynamic properties of Mimetic-Einstein-Gauss-Bonnet black hole, specifically focusing on parameters like temperature and entropy (see also the Joule–Thomson expansion in a mimetic black hole [71]). The first quantity we introduce is the temperature of the black hole, which is related to the surface gravity [70,71]. Using this correlation, the temperature of the black hole can be calculated through its surface gravity [72–74] as

$$T = \frac{\kappa_h}{2\pi} = \frac{1}{4\pi}\left(\frac{1}{\sqrt{|g_{tt}g_{rr}|}}\left|\frac{dg_{tt}}{dr}\right|\right)_{r=r_h}\,. \tag{3.1}$$

Based on the given metric function, the temperature function in our setup can be expressed as follows

$$T{=}\frac{A'(r)\mathrm{e}^{A(r)}}{4\pi\sqrt{\phi'^2(r)\mathrm{e}^{A(r)}}}\,. \tag{3.2}$$

Note that λ as the mimetic Lagrange multiplier shows itself via $A(r)$. In fact, the above-mentioned formula for spherically symmetric black holes is applicable in theories that include higher-order corrections, like the Gauss-Bonnet term. The final expression in the black hole temperature, equation (3.2), is obtained by substituting the values of the metric components g_{tt} and g_{rr} in the temperature formula (3.1). So the temperature of the black hole can be expressed solely in terms of the mimetic coefficient λ and the radial coordinate r, relying on the specific characteristics of the Einstein-Gauss-Bonnet theory and the attributes of the mimetic scenario. Once again, due to complexity of the relation for $A(r)$, there is no closed form analytical solution to the temperature. The entropy of the Mimetic-Einstein-Gauss-Bonnet black hole can be calculated through the Euclidean approach, resulting in the following equation [71,72,75]:

$$S = \beta\left[\frac{\partial(\beta F)}{\partial\beta} - F\right]. \tag{3.3}$$

Here, S represents the entropy, and F represents the Helmholtz free energy of the system which can be described within the framework of the Euclidean form of the action I_E, $\beta = \frac{1}{(\kappa_B T)}$ and $F = \frac{I_E}{\beta}$ [65,71].

The aforementioned equations are employed to calculate the asymptotic entropy of the black hole. However, in non-asymptotic states, these equations require modifications [65,74].

In this case, we may write

$$S=-2\pi\oint d^2x\sqrt{h_2}\Big(\frac{\partial L}{\partial R_{abcd}}\Big)_H\hat{\varepsilon}_{ab}\hat{\varepsilon}_{cd} \tag{3.4}$$

where L is the Lagrangian of the theory, $\hat{\varepsilon}_{ab}$ the binormal to the horizon surface H, and h_2 is the determinant of the 2-dimensional projected metric on H [71,72,75–77]. The similarity between the Euclidean and Noether charge approaches has been proven in [78]. Various methods have been employed to determine the entropy of stationary black holes. In this context, we compare the Noether charge method (valid for any Lagrangian theory that is invariant under diffeomorphisms) with various Euclidean techniques. Specifically, we examine (i) the microcanonical ensemble method suggested by Brown and York [79], (ii) the closely associated method introduced by Bañados, Teitelboim, and Zanelli, which expresses black hole entropy in terms of the Hilbert action surface term [80], (iii) an alternative formula by Bañados, Tetelboim, and Zanelli, also utilized by Susskind and Uglum, which treats black hole entropy as linked to a conical deficit angle [81], and (iv) the approach of pair creation proposed by Garfinkle, Giddings, and Strominger [82]. Each of these methods are limited in their applicability when compared to the Noether charge method [83]. This is especially the case in theories that include higher-order corrections such as the Gauss-Bonnet (GB) term. However, it is important to emphasize that the Noether charge method is commonly preferred for its efficiency in calculating black hole entropy [78]. Now, based on the variation of the Lagrangian (3.4) with respect to to the Riemann tensor and aforementioned points, we can express the entropy relationship as follows [53]:

$$\begin{aligned}S=-\frac{1}{8}\oint d^2x\sqrt{h_{(2)}}\Big\{\frac{1}{2}(g^{ac}g^{bd}-g^{bc}g^{ad})+f(\phi)\big[2R^{abcd}+2(g^{ac}R^{bd}-g^{bc}R^{ad}-g^{ad}R^{bc}+g^{bd}R^{ac})\\+R(g^{ac}g^{bd}-g^{bd}R^{ac})\big]\Big\}|_H\,\hat{\varepsilon}_{ab}\hat{\varepsilon}_{cd}\,.\end{aligned} \tag{3.5}$$

The first term in the brackets of this expression comes from the modification of the Einstein-Hilbert term. This expression can be computed to yield an optimal outcome as follows [67]

$$S_1=-\frac{1}{16}\oint d^2x\sqrt{h_{(2)}}(\hat{\varepsilon}_{ab}\hat{\varepsilon}^{cd}-\hat{\varepsilon}_{ab}\hat{\varepsilon}^{ab})\,. \tag{3.6}$$

We note that $\hat{\varepsilon}_{ab}$ is anti-symmetric and furthermore, complies with $\hat{\varepsilon}_{ab}\hat{\varepsilon}^{ab}=-2$. Hence, we achieve at the following well-known expression

$$S_1=\frac{A_H}{4}. \tag{3.7}$$

This equation depicts the horizon surface as $A_H=4\pi r_h^2$, with the other components in Equation (3.5) being directly related to the coupling function $f(\phi)$ and also affected by changes in the Mimetic term. In order to proceed the computation, it is noted that the binormal vector can be expressed on the horizon surface $\hat{\varepsilon}_{ab}=-\sqrt{-g_{00}g_{11}}|_H(\delta^0_a\delta^1_b-\delta^1_a\delta^0_b)$. This enables us to express the terms in a different form following Refs. [53]:

$$\Big(\frac{\partial L}{\partial R_{abcd}}\Big)_H\hat{\varepsilon}_{ab}\hat{\varepsilon}_{cd}=4g_{00}g_{11}|_H\Big(\frac{\partial L}{\partial R_{0101}}\Big)_H\,. \tag{3.8}$$

Hence, the terms that are directly related to $f(\phi)$ can be represented as follows:

$$S_2=-\frac{1}{2}f(\phi)g_{00}g_{11}|_H\oint d^2x\sqrt{h_{(2)}}\Big[2R^{0101}-2(g^{00}R^{11}-g^{10}R^{01}-g^{01}R^{10}+g^{11}R^{00})+g^{00}g^{11}R\Big]_H\,, \tag{3.9}$$

and therefore,

$$S_2 = \frac{f(\phi)A_H}{r_h^2} = 4\pi f(\phi)\,. \tag{3.10}$$

The obtained expression for the Mimetic-Einstein-Gauss-Bonnet (GB) black hole entropy confirms that the entropy is directly influenced by the form of the coupling function and the mimetic constraint. Nevertheless, the auxiliary field $\lambda(r)$ does influence various characteristics of the black hole in a quantitative way, such as its entropy and temperature as discussed in references [67,72–74]. Specially, we have

$$S_h = \frac{A_h}{4} + 4\pi f(\phi)\,. \tag{3.11}$$

The last term is specifically a trace of the mimetic scalar field coupled to the GB term.

4 Numerical Solutions

To achieve the black hole solutions in Einstein-Gauss-Bonnet gravity with mimetic constraint, we calculated the scalar field $\phi(r)$ and the metric components using the field equations, but we were not able to derive these parameters analytically in closed form due to complexity of the relation for $A(r)$. So, to proceed further, we resort to numerical methods to check the behavior of the mimetic field and other important quantities such as $\lambda(r)$. To preform our numerical study, we chose some specific forms for the coupling function $f(\phi(r))$.

To acquire solutions for mimetic black holes in the context of the Einstein-Gauss-Bonnet theory with the mimetic constraint, we derived the gravitational field equations and the equation for the scalar field. Because of the complexity of our equations as we said, obtaining closed analytical expressions for the metric and the scalar field in terms of r is not possible, leading to the use of numerical methods to investigate the field behavior. To better understand the behavior of the metric and to compare different scenarios, we can consider the following plots. Figure 1 illustrates the metric function's behavior at various radial coordinate from the event horizon (near the horizon and at asymptotic large distances)for mimetic black holes following Ref. [21], Mimetic-Gauss-Bonnet black hole (our setup), and the Schwarzschild black hole solution. We note that in our numerical analysis, we worked in the units where the horizon radius is normalized to unity. Specifically, for the metric function plotted in Figure 1, the horizon is located at $r_h = 1$ (in the adopted convention for the fundamental constants).

As shown in Figure 1, the Mimetic-Einstein-Gauss-Bonnet black hole, which is based on the Einstein-Gauss-Bonnet theory, exhibits a completely asymptotically flat behavior. It is noticed that near the black hole horizon, the temporal metric function approaches zero as usual, while the spatial metric component diverges and tends to infinity. Conversely, at distances far from the event horizon, this behavior is reversed, with both temporal and spatial metric components tending towards constant numerical values. By examining the graph, it is clear that, at very large distances, the metric functions satisfy the condition that $e^{A(r)} = e^{B(r)}$. At the large distances, the spacetime structure becomes flat and Minkowskian (without curvature). While in mimetic black hole, due to the influence of the mimetic gravitational effects, the metric may exhibit more complex behavior near the event horizon than what is predicted by the standard General Relativity. The Lagrange multiplier in mimetic black holes behaves like a perfect fluid with negative pressure, similar to the dark energy, and leads to significant spacetime curvature; see for instance Ref. [21]. For the sake of comparison, the plots we generated using the analytical results of the pure mimetic

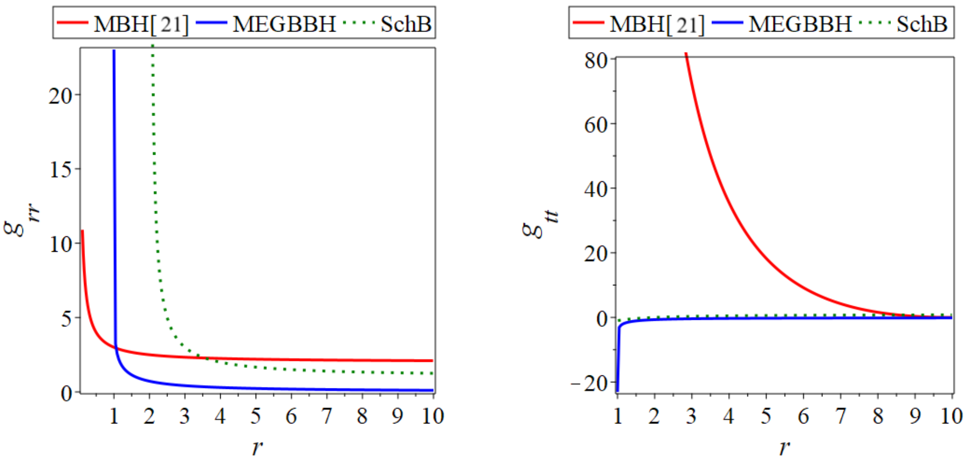

Figure 1: Left: g_{rr} and Right: g_{tt}; the components of the metric as a function of radial coordinate r. The red curve corresponds to the mimetic black hole (MBH), the blue curve represents the Mimetic-Einstein-Gauss-Bonnet black hole (MEGBBH), and the green curve shows the Schwarzschild black hole (SchB). We have set $r_h = 1$ in our adopted units.

case reported in Ref. [21] show that the time component of the metric increases near the event horizon, while the spatial component approaches a constant value. This behavior is in contrast to what is observed in the Schwarzschild black hole and the Mimetic Gauss-Bonnet black hole diagrams. In contrast, when examining a mimetic black hole within the context of the Gauss-Bonnet theory, we observe that the metric behaves asymptotically flat both near the horizon and at large distances. As is well known, the Gauss-Bonnet coupling function, which is related to gravitational corrections in spacetime, can modify the spacetime structure in various regions. One feature of the Gauss-Bonnet correction is that these models generally tend to exhibit flat behavior (asymptotic flatness) in the distant regions, as the additional gravitational effects diminish at large distances, and space-time approaches a flat state. The combination of mimetic effects and Gauss-Bonnet corrections can adjust and modify the gravitational behavior at large distances. Typically, these two effects can interact in such a way that the metric behaves asymptotically flat in the distant regions of the black hole. This interaction may occur due to the reduced gravitational effects at large distances and the dominance of mimetic and Gauss-Bonnet effects, leading to the metric ultimately becoming asymptotically flat.

We also use the Schwarzschild black hole metric [80]:

$$ds^2 = \left(1 - \frac{2M}{r}\right)dt^2 + \left(1 - \frac{2M}{r}\right)^{-1}dr^2 - r^2\left(d\theta^2 + \sin^2(\theta)d\phi^2\right), \tag{4.1}$$

and related quantities as a benchmark for analyzing and comparing the behavior of the Mimetic-Einstein-Gauss-Bonnet black hole. In Figure 1, we have shown also the metric behavior of the Schwarzschild black hole (SchB) from both time and space perspectives. Near the event horizon, it is observed that the time component experiences a significant contraction. In other words, for an external observer, time near the event horizon approaches zero. The spatial component, representing spacetime curvature, increases sharply near the event horizon. This indicates that spatial distances become so curved that; near the event horizon space-time is stretched to infinity. At large distances from the black hole, the time component approaches unity, indicating the normal passage of time, and the spatial component also approaches unity, signifying flat spacetime with no curvature.

Now, to study the behavior of the Lagrange multiplier $\lambda(r)$, we provide a short review of some required preliminaries. As mentioned earlier, several modified gravity models have recently been proposed to reproduce the gravitational effects of the dark matter. The variational principle in these models leads to more general equations of motion compared to standard General Relativity, making it possible to describe effective dark matter. The true nature of the dark matter is one of the main puzzles in modern cosmology, as it still avoids direct detection and reveals itself only through its gravitational influence at galactic and cosmological scales. Because of this, many researchers have tried to explain its observable effects by changing/modifiying or extending General Relativity. Within the mimetic scenario, in simpler versions of the mimetic dark matter model, the action is rewritten by adding a Lagrange multiplier $\lambda(r)$, as follows [9]:

$$S_{\pm} = \int d^4x\sqrt{-g}\left[\frac{R}{2} + \lambda(g^{\mu\nu}\partial_\mu\phi\partial_\nu\phi \mp 1)\right] . \tag{4.2}$$

As has been discussed in Introduction, taking the variation of the action with respect to $\lambda(r)$ gives the constraint:

$$g^{\mu\nu}\partial_\mu\phi\partial_\nu\phi = \pm 1 \, . \tag{4.3}$$

This shows that the mimetic model is equivalent to standard General Relativity with a scalar field that appears in the action only through this constraint. This simplified setup still keeps the full structure of the original model. The field $\lambda(r)$ can also be treated as a dynamical field with its own kinetic term and potential. If the scalar field $\phi(r)$ satisfies $\phi'(r) = 1$, then $\lambda(r)$ behaves like a^{-3}, which is the same scaling as the dark matter in an expanding universe, see Ref. [81] for more details. In the study of mimetic black holes in Ref. [21], the authors analyzed how $\lambda(r)$ changes with the radial coordinate r. They derived a differential equation for $\lambda(r)$ from the modified Einstein equations, and then solved and plotted it for the specific case with $c_0 = 2$ and $r_f = 4$. The result shows two singularities: one at $r = 0$, which is a usual curvature singularity, and another at $r = r_f$, which comes from the structure of the mimetic scalar field and is called a *caustic singularity.* The caustic-type singularity is a distinctive feature of the mimetic gravity framework. The plot of $\lambda(r)$ for MBH shows a branch cut at $r = r_f$, where $\lambda(r)$ changes sign in a discontinuous way, with $\lim \lambda(r) \to -\infty$ when $r \to r_f^+$ and $\lim \lambda(r) \to +\infty$ when $r \to r_f^-$. This indicates a sharp and asymmetric singularity at that point. In comparison, in the Schwarzschild solution of General Relativity, both the Ricci scalar and Ricci tensor are equal to zero. But in the mimetic gravity model, these curvature quantities are not zero. So, it makes sense to use them directly to study singularities, instead of focusing only on the Kretschmann scalar as one does in vacuum solutions. In comparison, for $\lambda(r)$ in our Mimetic-Einstein-Gauss-Bonnet model which is constructed by addition of the Gauss-Bonnet term to the pure Mimetic action, as shown in Figure 2, the caustic structures have been removed and only the real singularity at $r_h = 1$ remains in this generalized mimetic scenario.

We note that to analyze the numerical results, we must firstly solve field equations numerically and then plot the corresponding graphs. As previously mentioned, field equations include a coupling function, $f(\phi)$, for which we can consider various forms. As an example, scalar field plots can be generated based on the assumed coupling functions as illustrated in Figure 3. We studied multiple configurations for the function $f(\phi)$ and plotted the necessary parameters with comparison in different contexts. While we could not find closed, analytical form of the metric at large distances from the black hole horizon for various coupling functions $f(\phi)$, our numerical results ensure that its behavior is influenced by the shape of

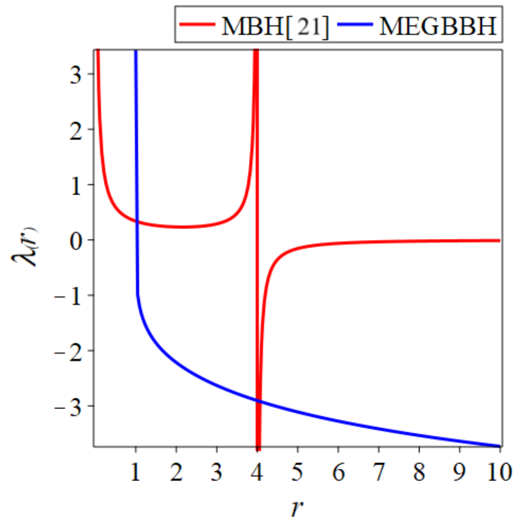

Figure 2: $\lambda(r)$ in terms of the radial coordinate r. The blue curve corresponds to the mimetic Einstein-Gauss-Bonnet black hole (MEGBBH), and the red curve represents the mimetic black hole (MBH). We have set $r_h = 1$ in our adopted units.

the coupling function $f(\phi)$. Figure 3 shows the behavior of $\phi(r)$ for three different coupling functions $f(\phi)$. Divergent or nonlinear coupling functions such as $f(\phi) = \alpha \log(\phi)$ (the red curves) can lead to instabilities. In the case where the coupling function is assumed to be logarithmic, the effect of the coupling term with the scalar field becomes significant primarily in regions of strong gravitational fields (e.g., near the horizon). However, at large distances where the space-time curvature decreases, the field no longer feels the influence of the coupling term. In the absence of other dynamical sources, it tends to approach its equilibrium value or zero. A sharp transition in the scalar field behavior is observed for forms such as $f(\phi) = \alpha\phi^3$ (the blue curve) or $f(\phi) = \alpha e^{\phi}$ (the green curve), where the field asymptotically approaches a finite value. In these cases, the scalar field is remarkably affected by the coupling function at the large distances, rising or falling further depending on the initial sign of the field.

5 Conclusion

In this work we have extended the framework of the mimetic black holes to the case where the Gauss-Bonnet effect is included. The theory is essentially a scalar-Einstein-Gauss-Bonnet gravity where the scalar degree comes from mimetic scenario. We derived all the necessary field equations along with attempt to solve them analytically. However, due to the complexity of the theory, closed-form, analytical solutions are not available in this setup. For instance, the analytical form of the metric function $A(r)$ even in some restricting conditions, can be achieved just in an integral form as Eq. (2.30) which has not closed-form solution. So, we were forced to study the theory's outcome numerically. The results with specific choices of the coupling function $f(\phi)$ are shown in figures. Indeed, our detailed calculations in the small r region have shown that the mimetic constraint around a typical black hole creates unique conditions for the ϕ parameter. Also, a gravitational singularity arises regardless of whether $\lambda(r)$ is positive or negative. Numerical analysis revealed that by adding

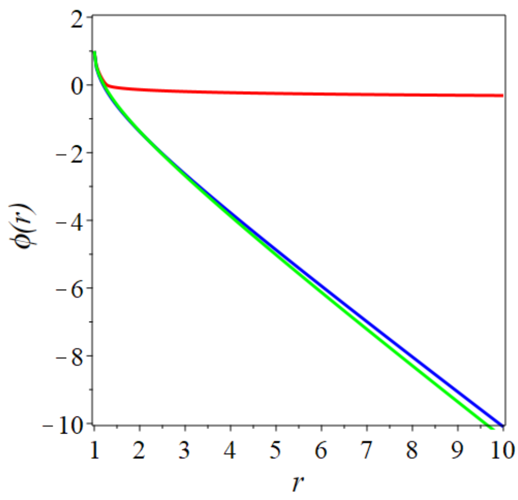

Figure 3: The scalar field $\phi(r)$ in terms of the radial coordinate r. The red line corresponds to $f(\phi) = \alpha \log \phi$, the blue line corresponds to $f(\phi) = \alpha\phi^3$ and the green line corresponds to $f(\phi) = \alpha e^{\phi}$.

the Gauss-Bonnet term to the action of the mimetic black hole as in our setup, the behavior of the metric function becomes asymptotically flat at large distances, and the structural singularities of the mimetic gravity are resolved. This is reasonable since Gauss-Bonnet effect has its origin in string theory as an approach to quantum gravity proposal with high energy (short distance) ultra-violet cutoff. However, these results were obtained only for a few specific forms of the coupling function, $f(\phi)$, which was assumed as a model parameter. In the calculations, λ was treated as a Lagrange multiplier that enters the Einstein equations and the metric functions; thus indirectly influencing the properties of this class of black holes. As an important result, we have shown that for $\lambda(r)$ in our Mimetic-Einstein-Gauss-Bonnet model, as shown in Figure 2, the caustic structures have been removed and only the real singularity at $r = 1$ remains in this generalized mimetic scenario. Detailed analysis has shown that when examining significant distances, black hole solutions in the framework of our field equations are well-defined, but the complex nature of the field equations makes it analytically impossible to determine such solutions in closed forms. So, we were forced to see the behavior of the solutions numerically. Examining the solutions at distances far from the event horizon, we found that the metric components exhibited constant behavior at infinite radial coordinate, while the Gauss-Bonnet constant term remained unchanged throughout space-time. The existence of mimetic constraint in a Gauss-Bonnet black hole with a scalar field can have an effect on various properties, such as entropy and temperature. The influence of the mimetic constraint on thermodynamic relationships has been treated via the metric components of the black hole solution, whereas the curvature of spacetime is determined by the mimetic constraint that appeared in the parameters of the Gauss-Bonnet black hole metric. To summarize, our study shows that various theoretical frameworks incorporating the Gauss-Bonnet term can produce novel black hole solutions, especially with a mimetic constraint.

Authors' Contributions

All authors have the same contribution.

Data Availability

The manuscript has no associated data or the data will not be deposited.

Conflicts of Interest

The authors declare that there is no conflict of interest.

Ethical Considerations

The authors have diligently addressed ethical concerns, such as informed consent, plagiarism, data fabrication, misconduct, falsification, double publication, redundancy, submission, and other related matters.

Funding

This research did not receive any grant from funding agencies in the public, commercial, or non-profit sectors.

Acknowledgment

We sincerely appreciate two anonymous referees for their very insightful and constructive comments that have boosted the quality of the manuscript remarkably.

References

[1] DESI Collaboration, "Data Release 1 of the Dark Energy Spectroscopic Instrument", [arXiv:2503.14745 [astro-ph.CO]].

[2] DESI Collaboration, "DESI DR2 Results II: Measurements of Baryon Acoustic Oscillations and Cosmological Constraints", [arXiv:2503.14738 [astro-ph.CO]].

[3] The Atacama Cosmology Telescope DR6, "The Atacama Cosmology Telescope: DR6 Constraints on Extended Cosmological Models", [arXiv:2503.14454 [astro-ph.CO]].

[4] A. H. Chamseddine and V. Mukhanov, "Mimetic dark matter", J. High Energy Phys. **2013**, 135 (2013) DOI: 10.1007/JHEP11(2013)135.

[5] A. H. Chamseddine and V. Mukhanov, "Resolving cosmological singularities", J. Cosmol. Astropart. Phys. **2017** (03), 9 (2017) DOI: 10.1088/1475-7516/2017/03/009.

[6] A. H. Chamseddine and V. Mukhanov, "Nonsingular black hole", Eur. Phys. J. C **77**, 183 (2017) DOI: 10.1140/epjc/s10052-017-4749-1.

[7] A. Casalino, M. Rinaldi, L. Sebastiani and S. Vagnozzi, "Mimicking dark matter and dark energy in a mimetic model compatible with GW170817", Phys. Dark Universe **22**, 108 (2018) DOI: 10.1016/j.dark.2018.10.001.

[8] A. Casalino, M. Rinaldi, L. Sebastiani and S. Vagnozzi, "Alive and well: Mimetic gravity and a higher-order extension in light of GW170817", Class. Quantum Gravity **36**, 17001 (2019) DOI: 10.1088/1361-6382/aaf186.

[9] A. H. Chamseddine, V. Mukhanov and A. Vikman, "Cosmology with Mimetic Matter", J. Cosmol. Astropart. Phys. **2014** (06), 17 (2014) DOI: 10.1088/1475-7516/2014/06/017.

[10] S. Capozziello, J. Matsumoto, S. Nojiri and S. Odintsov, "Dark energy from modified gravity with Lagrange multipliers", Phys. Lett. B **693**, 198 (2010) DOI: 10.1016/j.physletb.2010.08.026.

[11] N. Afshordi, A. Ashtekar, E. Barausse and E. Berti et al., "Black Holes Inside and Out 2024: visions for the future of black hole physics", [arXiv:2410.14414 [gr-qc]].

[12] S. Nojiri and S. D. Odintsov, "Mimetic $f(R)$ gravity: inflation, dark energy and bounce", [arXiv:1408.3561 [hep-th]].

[13] S. Nojiri, S. D. Odintsov and V. K. Oikonomou, "Modified gravity theories on a nutshell: Inflation, bounce and late-time evolution", Phys. Rep. **692**, 1 (2017) DOI: 10.1016/j.physrep.2017.06.001.

[14] N. Sadeghnezhad and K. Nozari, "Braneworld Mimetic Cosmology", Phys. Lett. B **769**, 134 (2017) DOI: 10.1016/j.physletb.2017.03.044.

[15] N. Hosseinkhan and K. Nozari, "Late time cosmological dynamics with a nonminimal extension of the mimetic matter scenario", Eur. Phys. J. Plus **133**, 50 (2018) DOI: 10.1140/epjp/i2018-11873-7.

[16] K. Nozari and N. Sadeghnezhad, "Braneworld mimetic $f(R)$ gravity", Int. J. Geom. Methods Mod. Phys. **16**, 1950042 (2019) DOI: 10.1142/S0219887819500428.

[17] K. Nozari and N. Rashidi, "Mimetic DBI Inflation in Confrontation with Planck2018 data", Astrophys. J. **882**, 68 (2019) DOI: 10.3847/1538-4357/ab3295.

[18] N. Rashidi and K. Nozari, "Viable intermediate inflation in the mimetic DBI model", Eur. Phys. J. C **81**, 834 (2021) DOI: 10.1140/epjc/s10052-021-09648-x.

[19] A. V. Astashenok, S. D. Odintsov and V. K. Oikonomou, "Modified Gauss-Bonnet gravity with the Lagrange multiplier constraint as mimetic theory", Class. Quantum Gravity **32**, 185007 (2015) DOI: 10.1088/0264-9381/32/18/185007.

[20] S. Nojiri, S. D. Odintsov and V. K. Oikonomou, "Viable mimetic completion of unified inflation-dark energy evolution in modified gravity", Phys. Rev. D **94**, 104050 (2016) DOI: 10.1103/PhysRevD.94.104050.

[21] M. A. Gorji, A. Allahyari, M. Khodadi and H. Firouzjahi, "Mimetic black holes", Phys. Rev. D **101**, 124060 (2020) DOI: 10.1103/PhysRevD.101.124060.

[22] S. Nojiri and G. G. L. Nashed, "Consistency between black hole and mimetic gravity- Case of (2+1)-dimensional gravity", Phys. Lett. B **830**, 137140 (2022) DOI: 10.1016/j.physletb.2022.137140.

[23] K. S. Stelle, "Renormalization of higher-derivative quantum gravity", Phys. Rev. D **16**, 953 (1977) DOI: 10.1103/PhysRevD.16.953.

[24] M. Tang and Z. Xu, "The no-hair theorem and black hole shadows", J. High Energy Phys. **2022**, 12 (2022) DOI: 10.1007/JHEP03(2022)012.

[25] H. Luckock and I. Moss, "Black holes have skyrmion hair", Phys. Lett. B **176**, 341 (1986) DOI: 10.1016/0370-2693(86)90172-1.

[26] M. S. Volkov and D. V. Galtsov, "Non-Abelian Einstein Yang-Mills black holes", JETP Lett. **50**, 346 (1989).

[27] J. D. Bekenstein, "Black holes with scalar charge", Ann. Phys. (N. Y). **91**, 75 (1975) DOI: 10.1016/0003-4916(75)90112-0.

[28] J. D. Bekenstein, "Novel 'no-scalar-hair' theorem for black holes", Phys. Rev. D **51**, R6608 (1995) DOI: 10.1103/PhysRevD.51.R6608.

[29] P. Kanti, N. E. Mavromatos, J. Rizos, K. Tamvakis and E. Winstanley, "Dilatonic black holes in higher curvature string gravity", Phys. Rev. D **54**, 5049 (1996) DOI: 10.1103/PhysRevD.54.5049.

[30] R. R. Metsaev and A. A. Tseytlin, "Order alpha-prime (two-loop) equivalence of the string equations of motion and the Sigma Model Weyl invariance conditions: Dependence on the dilaton and the antisymmetric tensor", Nucl. Phys. B **293**, 385 (1987) DOI: 10.1016/0550-3213(87)90077-2.

[31] G. W. Horndeski, "Second-order scalar-tensor field equations in a four-dimensional space", Int. J. Theor. Phys. **10**, 363 (1974) DOI: 10.1007/BF01807638.

[32] A. Nicolis, R. Rattazzi and E. Trincherini, "Galileon as a local modification of gravity", Phys. Rev. D **79**, 064036 (2009) DOI: 10.1103/PhysRevD.79.064036.

[33] L. Hui and A. Nicolis, "No-Hair Theorem for the Galileon", Phys. Rev. Lett. **110**, 241104 (2013) DOI: 10.1103/PhysRevLett.110.241104.

[34] T. P. Sotiriou and V. Faraoni, "Black Holes in Scalar-Tensor Gravity", Phys. Rev. Lett. **108**, 081103 (2012) DOI: 10.1103/PhysRevLett.108.081103.

[35] T. P. Sotiriou and S.-Y. Zhou, "Black Hole Hair in Generalized Scalar-Tensor Gravity", Phys. Rev. Lett. **112**, 251102 (2014) DOI: 10.1103/PhysRevLett.112.251102.

[36] E. Babichev and C. Charmousis, "Dressing a black hole with a time-dependent Galileon", J. High Energy Phys. **2014**, 106 (2014) DOI: 10.1007/JHEP08(2014)106.

[37] D. D. Doneva and S. S. Yazadjiev, "New Gauss-Bonnet Black Holes with Curvature-Induced Scalarization in Extended Scalar-Tensor Theories", Phys. Rev. Lett. **120**, 131103 (2018) DOI: 10.1103/PhysRevLett.120.131103.

[38] C. A. R. Herdeiro and E. Radu, "Asymptotically flat black holes with scalar hair: a review", [arXiv:1504.08209 [gr-qc]].

[39] P. A. González, E. Papantonopoulos, J. Saavedra and Y. Vásquez, "Extremal hairy black holes", J. High Energy Phys. **2014**, 1 (2014) DOI: 10.1007/JHEP12(2014)001.

[40] S. R. Dolan, S. Ponglertsakul and E. Winstanley, “Stability of black holes in Einstein-charged scalar field theory in a cavity”, Phys. Rev. D **92**, 124047 (2015) DOI: 10.1103/PhysRevD.92.124047.

[41] D. Lovelock, “The Einstein tensor and its generalizations”, J. Math. Phys. **12**, 498 (1971) DOI: 10.1063/1.1665613.

[42] C. A. Lanczos, “Remarkable Property of the Riemann-Christoffel Tensor in Four Dimensions”, Ann. Math. **39**, 842 (1938) DOI: 10.2307/1968467.

[43] D. G. Boulware and S. Deser, “String-Generated Gravity Models”, Phys. Rev. Lett. **55**, 2656 (1985) DOI: 10.1103/PhysRevLett.55.2656.

[44] R. C. Myers and J. Z. Simon, “Black-hole thermodynamics in Lovelock gravity”, Phys. Rev. D **38**, 2434 (1988) DOI: 10.1103/PhysRevD.38.2434.

[45] Y. M. Cho and I. P. Neupane, “Anti-de Sitter black holes, thermal phase transition, and holography in higher curvature gravity”, Phys. Rev. D **66**, 024044 (2002) DOI: 10.1103/PhysRevD.66.024044.

[46] C. Sahabandu, P. Suranyi, C. Vaz and L. C. R. Wijewardhana, “Thermodynamics of static black objects in D dimensional Einstein-Gauss-Bonnet gravity with $D-4$ compact dimensions”, Phys. Rev. D **73**, 044009 (2006) DOI: 10.1103/PhysRevD.73.044009.

[47] A. Kumar, D. V. Singh and S. G. Ghosh, “Hayward black holes in Einstein-Gauss-Bonnet gravity”, Ann. Phys. **419**, 168214 (2020) DOI: 10.1016/j.aop.2020.168214.

[48] S. G. Ghosh and S. D. Maharaj, “Cloud of strings for radiating black holes in Lovelock gravity”, Phys. Rev. D **89**, 084027 (2014) DOI: 10.1103/PhysRevD.89.084027.

[49] S. Capozziello and G. G. L. Nashed, “Charged spherically symmetric black holes in scalar-tensor Gauss-Bonnet gravity”, Class. Quantum Gravity **40**, 205023 (2023) DOI: 10.1088/1361-6382/acf2d0.

[50] A. Sheykhi, “Mimetic gravity in $f(R)$-dimensions”, J. High Energy Phys. **2021**, 043 (2021) DOI: 10.1007/JHEP01(2021)043.

[51] L. Sebastiani, S. Vagnozzi and R. Myrzakulov, “Mimetic Gravity: A Review of Recent Developments and Applications to Cosmology and Astrophysics”, Adv. High Energy Phys. **2017**, 3156915 (2017) DOI: 10.1155/2017/3156915.

[52] J. Kaplan and J. Wang, “An Effective Theory for Holographic RG Flows”, [arXiv:1406.4152 [hep-th]].

[53] N. Behr and A. Mukhopadhyay, “Holography as a highly efficient renormalization group flow. I. Rephrasing Gravity”, Phys. Rev. D **94**, 026001 (2016) DOI: 10.1103/PhysRevD.94.026001.

[54] N. Behr and A. Mukhopadhyay, “Holography as a highly efficient renormalization group flow. II. An explicit construction”, Phys. Rev. D **94**, 026002 (2016) DOI: 10.1103/PhysRevD.94.026002.

[55] H. Adami, M. M. Sheikh-Jabbari and V. Taghiloo, “Gravity Is Induced By Renormalization Group Flow”, [arXiv:2508.09633 [hep-th]].

[56] I. Papadimitriou, “Lectures on Holographic Renormalization”, in Theoretical Frontiers in Black Holes and Cosmology, Springer Proc. Phys. **176**, 131 (2016) DOI: 10.1007/978-3-319-31352-8_4.

[57] K. Skenderis, “Lecture Notes on Holographic Renormalization”, Class. Quantum Gravity **19**, 5849 (2002) DOI: 10.1088/0264-9381/19/22/306.

[58] B.-B. Wei, Z.-F. Jiang and R.-B. Liu, “Thermodynamic holography”, Sci. Rep. **5**, 15077 (2015) DOI: 10.1038/srep15077.

[59] K. L. Panigrahi and B. Singh, “Holographic Extended Thermodynamics of deformed AdS-Schwarzschild black hole”, [arXiv:2508.14873 [hep-th]].

[60] M. Zhang et al., “Finite-cutoff Holographic Thermodynamics”, [arXiv:2507.01010 [hep-th]].

[61] B. Pourhassan et al., “Holographic Thermodynamics of an Enhanced Charged AdS Black Hole in String Theory’s Playground”, J. Hologr. Appl. Phys. **4**, 15 (2024).

[62] B. Pourhassan and S. Upadhyay, Thermodynamics of Quantum Black Holes: Holography, Damghan University Press, 2024.

[63] A. Bakopoulos, G. Antoniou and P. Kanti, “Novel black-hole solutions in Einstein-scalar-Gauss-Bonnet theories with a cosmological constant”, Phys. Rev. D **99**, 064003 (2019).

[64] G. Nashed, “Charged and Non-Charged Black Hole Solutions in Mimetic Gravitational Theory”, Symmetry **10**, 559 (2018).

[65] C. Tsallis and L. J. L. Cirto, “Black hole thermodynamical entropy”, Eur. Phys. J. C **73**, 2487 (2013).

[66] F. Bajardi, K. F. Dialektopoulos and S. Capozziello, “Higher Dimensional Static and Spherically Symmetric Solutions in Extended Gauss–Bonnet Gravity”, Symmetry **12**, 372 (2020).

[67] G. Antoniou, A. Bakopoulos and P. Kanti, “Black-Hole Solutions with Scalar Hair in Einstein-Scalar-Gauss-Bonnet Theories”, Phys. Rev. D **97**, 084037 (2018).

[68] A. Bakopoulos *et al.*, “Black holes with primary scalar hair”, Phys. Rev. D **109**, 024032 (2024).

[69] A. Sheykhi and S. Grunau, “Topological black holes in mimetic gravity”, Int. J. Mod. Phys. A **36**, 2150186 (2021).

[70] G. G. L. Nashed and S. Nojiri, “Black holes with Lagrange multiplier and potential in mimetic-like gravitational theory: multi-horizon black holes”, J. Cosmol. Astropart. Phys. **2022**, 011 (2022).

[71] A. H. Rezaei and K. Nozari, “Joule–Thomson expansion in a mimetic black hole”, Sci. Rep. **14**, 19475 (2024).

[72] M. Cvetič and S. Nojiri, “Black hole thermodynamics and negative entropy in de Sitter and anti-de Sitter Einstein-Gauss-Bonnet gravity”, Nucl. Phys. B **628**, 295 (2002).

[73] D. V. Singh, V. Bhardwaj and S. Upadhyay, “Thermodynamic properties, thermal image and phase transition of Einstein-Gauss-Bonnet black hole coupled with nonlinear electrodynamics”, Eur. Phys. J. Plus **137**, 126 (2022).

[74] G. W. Gibbons and R. E. Kallosh, “Topology, entropy, and Witten index of dilaton black holes”, Phys. Rev. D **51**, 2839 (1995).

[75] S. W. Hawking and D. N. Page, “Thermodynamics of black holes in anti-de Sitter space”, Commun. Math. Phys. **87**, 577 (1983).

[76] J. W. York, “Black hole in thermal equilibrium with a scalar field: The back-reaction”, Phys. Rev. D **31**, 775 (1985).

[77] A. Teimouri, “Entropy of non-local gravity”, [arXiv:1705.11164 [hep-th]].

[78] V. Iyer and R. M. Wald, “Some properties of the Noether charge and a proposal for dynamical black hole entropy”, Phys. Rev. D **50**, 846 (1994).

[79] J. D. Brown and J. W. York, “The Microcanonical functional integral. 1. The Gravitational field”, Phys. Rev. D **47**, 1420 (1993).

[80] M. Bañados, C. Teitelboim and J. Zanelli, “The Black Hole in Three Dimensional Space Time”, Phys. Rev. Lett. **69**, 1849 (1992).

[81] L. Susskind and J. Uglum, “Black Hole Entropy in Canonical Quantum Gravity and Superstring Theory”, Phys. Rev. D **50**, 2700 (1994).

[82] D. Garfinkle, S. B. Giddings and A. Strominger, “Entropy in Black Hole Pair Production”, Phys. Rev. D **49**, 958 (1994).

[83] J. Diaz-Alonso and D. Rubiera-Garcia, “Thermodynamic analysis of black hole solutions in gravitating nonlinear electrodynamics”, Gen. Relativ. Gravit. **45**, 1901 (2013).